Dissolved organic matter and the glacial-interglacial pCO 2 problem

Didier Paillard, Michael Ghil, Hervé Le Treut

GLOBAL BIOGEOCHEMICAL CYCLES, VOL. 7, NO. 4, PAGES 901-914, DECEMBER 1993

DISSOLVED ORGANIC MATTER AND THE GLACIAL-INTERGLACIAL pCO_2 PROBLEM

Didier Paillard[1]

Laboratoire de Modélisation du Climat et de l'Environnement, CEA-DSM, Centre d'études de Saclay, Orme des merisiers, Gif-sur-Yvette, France

Michael Ghil

Department of Atmospheric Sciences and Institute of Geophysics and Planetary Physics, University of California, Los Angeles

Hervé Le Treut

Laboratoire de Météorologie Dynamique, Ecole Normale Supérieure, Paris, France

Abstract. Two box models, one analytical and one numerical, are used to investigate systematically a broad range of oceanic circulation changes on the atmospheric carbon dioxide (CO_2) concentration. A number of oceanic carbon cycle models have failed to reproduce the 30% increase in CO_2 partial pressure (pCO_2) during the last deglaciation as reconstructed from polar ice cores. We apply therefore this approach of exploring the model's parameter space to examine the effect of long-lived dissolved organic matter on the system. The results from the two models complement each other, in terms of insight versus detail. Carbon is usually assumed to be transported from the surface into the deep ocean through the sedimentation of particulate matter. If there exists in the ocean a pool of dissolved organic matter (DOM) with a regeneration time comparable with the advection time, then the associated carbon can also be advected, resulting in a different distribution. Such a DOM reservoir acts as a smoother on the spatial distribution of nutrients in the sea, particularly in the equatorial intermediate waters. We establish the role of intermediate waters as one of the key components of the oceanic carbon cycle and show that DOM reduces the sensitivity of the carbon cycle to oceanic circulation pattern changes, mainly because of its smoothing effect. Consequently, the possible existence of DOM species with a time constant of the order of a century tends to reduce, rather than enhance, the glacial-interglacial difference in pCO_2 levels due to changes in the thermohaline circulation.

[1]Also at Centre des Faibles Radioactivités, Domaine du CNRS, Gif sur Yvette, France.

Paper number 93GB02013.
0886-6236/93/93GB-02013$10.00

1. INTRODUCTION

The analysis of air bubbles trapped in polar ice has revealed that the atmospheric concentration of carbon dioxide (CO_2) was approximately 30% lower during the last glacial maximum than during preindustrial time [Barnola et al., 1987; Delmas et al., 1980]. Such a decrease in greenhouse gas concentration may be responsible for as much as half of the temperature difference between a glacial age and today. It is therefore important to understand the origin of this variability in the CO_2 partial pressure pCO_2.

The ocean being the largest reservoir of carbon able to exchange CO_2 with the atmosphere on timescales shorter than a few thousands of years, it has been proposed that these pCO_2 variations are the result of changes in the oceanic circulation or in the ocean's biological productivity. This view is further supported by $^{13}C/^{12}C$, Cd/Ca and calcium carbonate dissolution records, which indicate considerable reorganization of the ocean's geochemistry and circulation during this time interval [Boyle, 1992; Broecker et al., 1990; Curry and Lohmann, 1983; Duplessy et al., 1988]. Simple box models of the ocean [Ghil et al., 1987; Stommel, 1961; Welander, 1988], as well as more elaborate, but still idealized ones [Quon and Ghil, 1992; Thual and McWilliams, 1992] also show that the thermohaline circulation can easily flip from one steady state circulation to a completely different one. The sensitivity of the carbon cycle to the ocean's circulation changes is therefore of considerable interest.

Numerous box models have been formulated in order to understand the basic mechanisms involved, from models with only three or four boxes [Knox and McElroy, 1984; Lyle and Pisias, 1990; Marino et al., 1992; Sarmiento and Toggweiler, 1984; Siegenthaler and Wenk, 1984] to models including approximately 15 boxes representing the major ocean water masses [Keir, 1988; Michel, 1992]. Three-dimensional ocean general circulation models (GCMs) have also been employed to

understand the problem of this glacial-interglacial difference in atmospheric carbon dioxide [Heinze et al., 1991; Maier-Reimer and Hasselmann, 1987]. However, depending on the model, only a 20-30 ppm difference, at best, can be explained, and therefore no model or mechanism has given a satisfactory explanation for the the 80-90 ppm documented difference.

In all these models it was assumed that the transit of organic matter in the water column was the result of falling particulate matter. However Sugimura and Suzuki [1988], using a new measurement method, have reported levels of dissolved organic matter (DOM) at intermediate levels in the water column several times higher than what was commonly expected — "standard" techniques yield surface water concentrations of dissolved organic carbon which fall in the 60-90 μmol L^{-1} range, while the new technique gives concentrations around 300 μmol L^{-1} near the surface and still above 100 μmol L^{-1} up to 500 m deep. The idea that organic matter may not only be falling down to the bottom of the ocean but also be advected horizontally seems to produce modeling results in better agreement with nutrient concentrations measured in the sea [Bacastow and Maier-Reimer, 1991; Toggweiler, 1988]. It is therefore tempting to look at the effect of organic matter on the glacial age pCO_2 problem.

In section 2 of this paper a three-box model is formulated in order to investigate the role of the different oceanic-circulation parameters. Using simple analytical formulae, we show that the vertical distribution of nutrients is a key to understand the relationship between the ocean's deep circulation and atmospheric pCO_2. The existence of a nutrient maximum in intermediate waters, as seen in today's ocean, implies a carbon reservoir just a few hundred meters below the sea surface and is associated with high atmospheric pCO_2. During glacial time, the slow-down of the general deep circulation reduces this nutrient maximum. The carbon's presence at greater depth in the water column lowers the atmospheric pCO_2. This mechanism depends on the regeneration of particulate organic matter in intermediate waters; hence introducing DOM into the model tends to reduce the effect oceanic circulation changes can have on atmospheric pCO_2, as seen in section 3.

The results in these two sections are mostly qualitative, so we introduce a four-box model in section 4 to obtain numerical estimates of the effect described above. A glacial-interglacial pCO_2 difference of 20-30 ppm can be obtained in the DOM-free version of the model; this is fairly close to most other model results in the litterature. The addition of DOM, which acts as a smoother on the vertical nutrient distribution, gives results in the 10-20 ppm range, and makes the glacial-interglacial pCO_2 problem more difficult.

2. THREE-BOX ANALYTICAL MODEL

2.1. *Model Description*

We describe here a simple model with only one surface box, an intermediate box and a deep box, in order to understand the relative role of the global thermohaline deep circulation (the parameter d), the upwellings (u), the vertical diffusion in the water column (the mixing m) and the biological production (see Figure 1). A separate polar-water box, the importance of which has been demonstrated by Sarmiento and Toggweiler [1984], is introduced in section 4. The schematic diagram of Figure 1 represents the simplest version of a two-stage extension of Broecker's [1982] bio pump, designed to explore the role of intermediate waters as a key link between the thermohaline circulation and the atmospheric CO_2 concentration. Two versions of this three-box model are considered: with and without DOM.

In order to estimate the equilibrium atmospheric pCO_2 we need to know the dissolved inorganic carbon concentration (DIC) and the alkalinity of the surface box. We also need to assume a simple relationship between the new production (P) and the concentration of limiting nutrient in the surface layer. We have therefore nine variables in the DOM-free version of

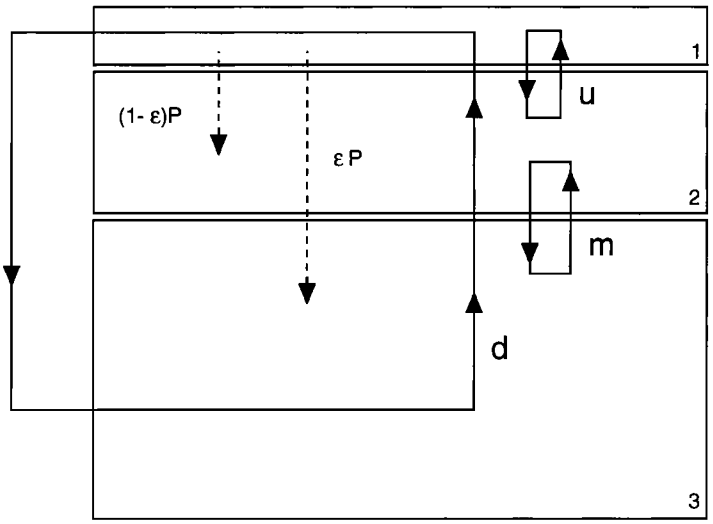

Fig. 1. Schematic diagram of the three boxes for the analytical model. The oceanic circulation is represented though the three circuits with fluxes d, u, and m, respectively. The new production P is a function of the nutrients in the surface box, and ε is the fraction of this production reaching the deep box by sedimentation.

the model: the nutrient content N_1, N_2, N_3, the alkalinity A_1, A_2, A_3, and the DIC content C_1, C_2, C_3 of each box: 1, surface; 2, intermediate; 3, deep. These variables obey the three following global conservation equations:

$$v_1 N_1 + v_2 N_2 + v_3 N_3 = N\,, \tag{1a}$$

$$v_1 A_1 + v_2 A_2 + v_3 A_3 = A\,, \tag{1b}$$

$$v_1 C_1 + v_2 C_2 + v_3 C_3 = C\,, \tag{1c}$$

where v_i is the the ratio of the volume of box i to the total volume of the ocean and N, A, and C are the mean value of the nutrient, alkalinity and DIC concentrations in the sea.

In this model the river input compensate exactly for the sedimentary output, and consequently the mean values N, A, and C are assumed to be constant. From the nine equations describing, for each concentration, the balance between sources and sinks in each box, any subset of six equations will be independent. The equilibrium values of all nine variables can then be found by solving, in addition to (1a)-(1c), for example the six equations corresponding to the surface and the deep box:

$$(u + d)(N_2 - N_1) - P = 0, \tag{2a}$$

$$d(N_1 - N_3) + m(N_2 - N_3) + \varepsilon P = 0, \tag{2b}$$

$$(u + d)(A_2 - A_1) - (2r_{ca} - r_n) P = 0, \tag{2c}$$

$$d(A_1 - A_3) + m(A_2 - A_3) + (2r_{ca}\varepsilon' - r_n \varepsilon) P = 0, \tag{2d}$$

$$(u + d)(C_2 - C_1) - (r_c + r_{ca}) P = 0\,, \tag{2e}$$

$$d(C_1 - C_3) + m(C_2 - C_3) + (r_c \varepsilon + r_{ca} \varepsilon') P = 0\,, \tag{2f}$$

where the nutrients and the biological production P are in phosphate units, r_n, r_{ca}, and r_c are the Redfield ratios for nitrate, calcite and organic carbon respectively (i.e., the "stoechiometric coefficients" of organic matter with respect to phosphate), ε is the fraction of the new production P reaching the deep box before being oxydized (of the order of 10% - 20%), and ε' is the fraction of the calcite produced ($r_{ca} P$) reaching the deep box before being dissolved (of the order of 90%). The DIC balance takes into account both "soft" and "hard" components of the new production ($r_c P$ and $r_{ca} P$ respectively), and the alkalinity balance both the contributions of $CO_3^=$ ions ($2\, r_{ca} P$) and of nitrate ($-\, r_n P$).

To incorporate DOM, we need the three additional variables D_1, D_2, D_3 representing its concentration in each box (in phosphate units), along with the corresponding conservation equations:

$$(u + d)(D_2 - D_1) - \frac{v_1}{\tau} D_1 + Q = 0\,, \tag{3a}$$

$$(m + d)(D_3 - D_2) + u(D_3 - D_2) - \frac{v_2}{\tau} D_2 = 0\,, \tag{3b}$$

$$d(D_1 - D_3) + m(D_2 - D_3) - \frac{v_3}{\tau} D_3 = 0\,, \tag{3c}$$

where τ is the time constant for DOM regeneration, and Q is the part of the biological production going into dissolved form. Equations (2a)-(2f) must be changed to

$$(u + d)(N_2 - N_1) - P + \frac{v_1}{\tau} D_1 - Q = 0\,, \tag{4a}$$

$$d(N_1 - N_3) + m(N_2 - N_3) + \varepsilon P + \frac{v_3}{\tau} D_3 = 0, \tag{4b}$$

$$(u + d)(A_2 - A_1) - (2r_{ca} + r_n) P - r_n \left(\frac{v_1}{\tau} D_1 - Q\right) = 0, \tag{4c}$$

$$d(A_1 - A_3) + m(A_2 - A_3) + (2r_{ca}\varepsilon' - r_n \varepsilon) P - r_n \frac{v_3}{\tau} D_3 = 0\,, \tag{4d}$$

$$(u + d)(C_2 - C_1) - (r_c + r_{ca}) P + r_c \left(\frac{v_1}{\tau} D_1 - Q\right) = 0, \tag{4e}$$

$$d(C_1 - C_3) + m(C_2 - C_3) + (r_c \varepsilon + r_{ca} \varepsilon') P + r_c \frac{v_3}{\tau} D_3 = 0\,, \tag{4f}$$

where we assume that Redfield ratios are the same for organic and particulate matter.

2.2. *The Nutrient Profile*

In order to establish the importance of intermediate waters for the atmospheric pCO_2, we discuss first the structure of the nutrient profile. Rearranging (2a) and (2b) gives

$$N_2 - N_3 = \left[\frac{d}{d+u} - \varepsilon\right] \frac{P}{d+m}\,. \tag{5}$$

The existence of a nutrient maximum in intermediate waters (i.e. $N_2 > N_3$), as seen in today's ocean, is the result of ε being smaller than $d/(d+u)$. Conversely, in order to get a deep ocean rich in nutrients, as the geological records suggest for glacial time [Boyle and Keigwin, 1982; Duplessy et al., 1988; Kallel et al., 1988], we can either increase the upwellings u, decrease the general circulation d, or increase the proportion ε of particulate organic matter reaching the deep ocean (see Figure 2). All three possibilities are compatible with current reconstructions of past ocean circulation and paleoproductivity. They may therefore very well act together to change the distribution of nutrients in the sea. Still, to eliminate this nutrient maximum, the values needed for ε, d, and u are very different from their present magnitudes. On the scale of the Atlantic Ocean a reasonable estimate for d, corresponding mainly to North Atlantic Deep Water (NADW), would be around 15 or 20 Sv (1 Sv = 10^6 m^3/s), and for u, near 5 or 10 Sv.

To represent the whole world ocean, we should add to d the Antarctic Bottom Water (AABW), about 20 Sv, and the upwelling in the Indian and in the Pacific Ocean. In either case, d is larger than u. On the other hand, ε varies greatly from one place to another (from approximately 1% in the open ocean to more than 20% along continental margins [Berger et al., 1989]) and from one season to the other (in mid-latitudes, ε is much larger during spring blooms, when the phytoplankton population increases dramatically, while the grazer population is still quite low). However, even with enhanced upwelling stimulating the productivity near the equator and along the continents, or with more violent spring blooms resulting from more brutal changes in the seasonal thermocline depth, it seems hard to believe that the value of ε can become as high as 30% or 40%. Even so, d would have to be no larger than roughly one third of u (for example, 5 Sv of NADW formation against 15 Sv of upwelling). As we will see later on, the addition of a polar box softens this conclusion, and less dramatic changes are needed to achieve a plausible geochemical simulation of the glacial-age ocean. Nevertheless, this simple relationship between ε, d, and u shows us that only major changes in the ocean circulation or in the productivity can account for the paleodata from deep-sea cores.

Including DOM, (5) is replaced by

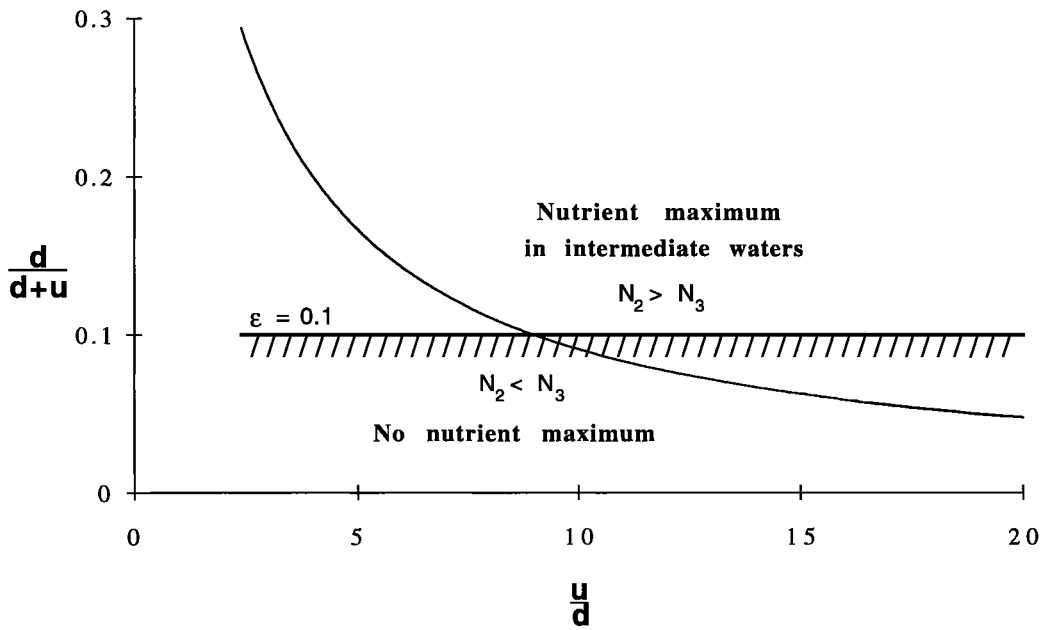

Fig. 2. Plot of the term $d/(d+u)$ in (5), compared with the fraction ε of organic matter reaching the deep ocean. The nutrient maximum of intermediate waters can disappear when the ratio u/d is large enough compared with ε.

$$N_2 - N_3 = \left[\frac{d}{d+u} - \varepsilon\right] \frac{P}{d+m} - (D_2 - D_3), \quad (6a)$$

$$D_2 - D_3 = G(d,u,m)\, Q, \quad (6b)$$

where $G(d,u,m)$ is a rational function of d, m, u, whose exact expression is given in Appendix A; its first-order behavior is given by

$$G(d,u,m) \sim \frac{u - \frac{v_2}{v_3} d}{(d+u)\left(\frac{d+m}{\lambda} + \frac{v_2}{\tau}\right)}, \quad (7)$$

where λ is the ratio $v_3/(v_2+v_3)$ (approximately 0.75 for an intermediate box of depth 1000 m and a total ocean depth of 4000 m). The sign of G is the sign of $[\, u - (v_2/v_3)\, d\,]$ in (7) as well as in the exact expression. For a 1000-m-deep intermediate box and a 4000-m-deep ocean, $(v_2/v_3) = 0.33$ and G is positive for reasonable present-day values of u (5-10 Sv) and d (15-20 Sv). Consequently, the nutrient maximum ($N_2 - N_3$) decreases when the DOM production Q increases. Hence DOM acts as a smoother on the vertical nutrient distribution. In an ice-age scenario, with u higher than at present and d lower, the value of G will be larger, and the "smoothing effect" of DOM more significant (see Figure 3). This will affect the sensitivity of atmospheric pCO_2 to oceanic-circulation changes during a glacial-interglacial transition.

2.3. *Atmospheric CO_2*

This simple three-box model does not include explicitly the atmosphere. However, since it has only one surface box, the carbon dioxide in the atmosphere will equilibrate with the DIC in this box; the resulting equilibrium partial pressure of CO_2 will be the same in the atmosphere and in the surface waters. Consequently, pCO_2 can be calculated from the temperature, salinity, alkalinity and carbon content of the surface box. This can be done exactly, but the purpose of this simple model is to show how the pCO_2 varies when parameters change, rather than give a precise numerical value for given parameter settings.

For a given temperature and a given salinity, Figure 4a shows that the equilibrium pCO_2 of the water increases with the DIC concentration minus the alkalinity. On this diagram, the slope of the isolines is close to 1.2, so that pCO_2 is, to first order, a decreasing function of $(A_1 - 1.2\, C_1)$, or equivalently an increasing function of $(C_1 - 0.8\, A_1)$. This function behaves exponentially. For t = 15°C and S = 35 ‰, the approximate formula is

$$pCO_2 \approx 144\ e^{4.2\,(C_1 - 0.8\,A_1)} \quad (8)$$

The relative errors in pCO_2 when using (8) versus the exact values are shown in Figure 4b. Oceanic values for carbon and alkalinity lie close to the main diagonal of Figures. 4a and 4b. For these C and A values the error in using (8) is less than 10% or even 5%.

With this simplification, and knowing the values of A_1 and C_1 from (1) and (2), we get

pCO_2 "increases with" $(C_1 - \mu\, A_1)$.

where $\mu = 0.8$. This yields, according to (1a)-(1c) and (2c)-(2f), that

pCO_2 "increases with"

$$-\left[r_c - (2\mu - 1) r_{ca} + \mu\, r_n\right] \frac{P}{d+u} \left[1 - \lambda \frac{d}{d+m}\right] \quad (9a)$$

$$+\ \lambda\ \left[(2\mu - 1) r_{ca}\, \varepsilon' - (r_c + \mu\, r_n)\, \varepsilon\right] \frac{P}{d+m}.$$

From Redfield ratios following Broecker and Peng [1982], i.e., $r_c = 106$, $r_{ca} = 21$ and $r_n = 15$, along with $\varepsilon = 0.1$ and $\varepsilon' = 0.9$, one has

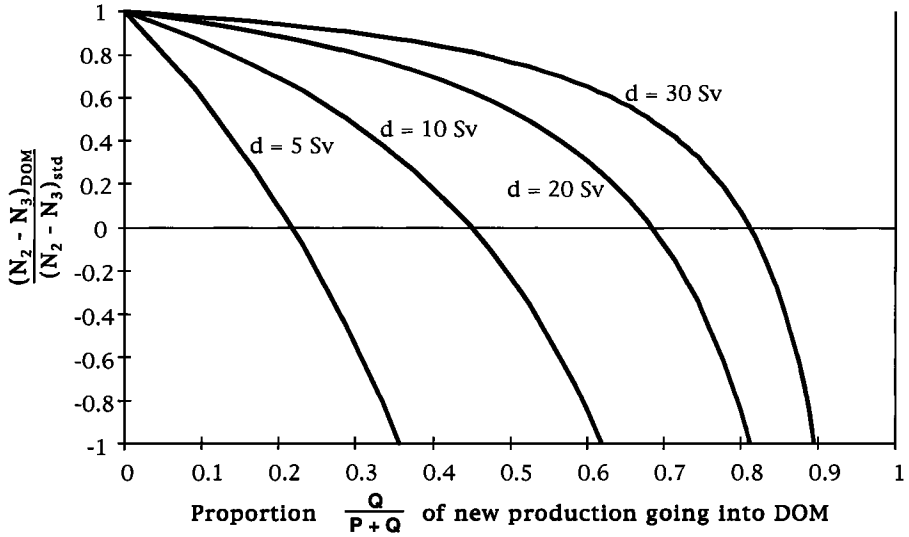

Fig. 3. Plot of the nutrient content in intermediate waters, normalized to the no-DOM situation, as a function of DOM production, compared to particulate production. When the deep circulation d is small (5 Sv), the nutrient maximum disappears as soon as approximately 30% of the new production is exported as DOM.

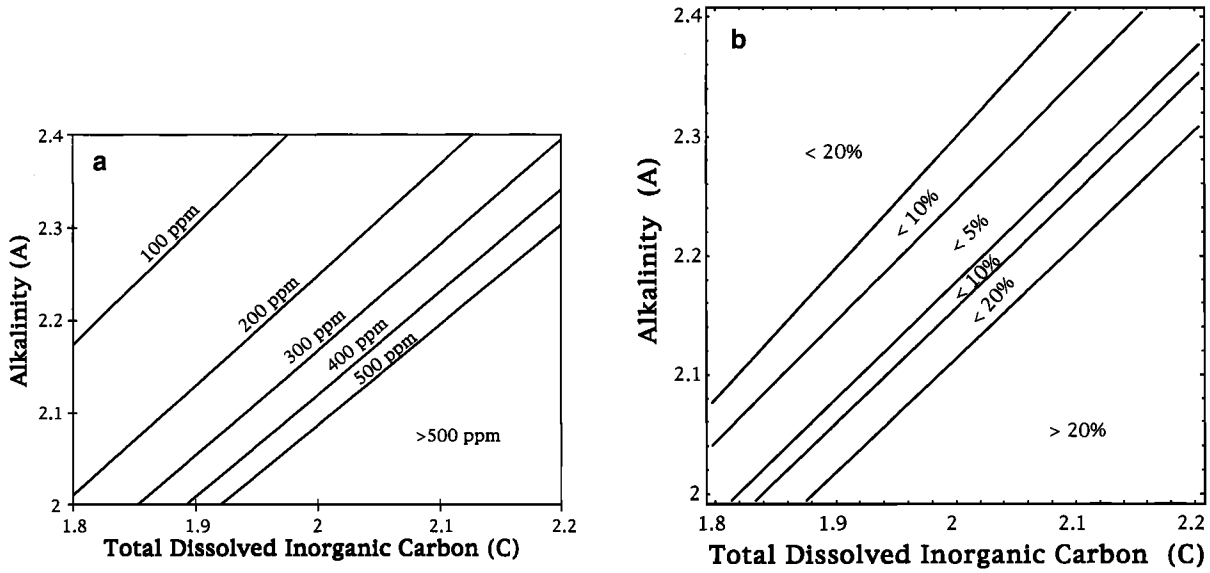

Fig. 4. (a) Plot of pCO_2 in surface waters as a function of total dissolved inorganic carbon C and alkalinity A, calculated from the chemical equilibrium at a given salinity of 35‰ and a temperature of 15°C. Note that, to first order, pCO_2 behaves like the carbon concentration C minus the alkalinity A. (b) Relative error in pCO_2 values when using the approximate equation (8), instead of the exact dependence of pCO_2 on C and A used in the four-box model.

$$[r_c - (2\mu - 1)r_{ca} + \mu\, r_n] \approx 105,$$

$$[(2\mu - 1)r_{ca}\, \varepsilon' - (r_c + \mu\, r_n)\, \varepsilon] \approx -0.5\ .$$

The final result is that

$$pCO_2 \text{ "increases with" } -105\,\frac{P}{d+u} + 105\,\lambda\,\frac{P}{d+u}\,\frac{d}{d+m} - 0.5\,\lambda\,\frac{P}{d+m}\ . \qquad (9b)$$

The term $P/(d+u)$ represents the effect of the biological pump compared to the upwelling of carbon-rich intermediate waters. The term $P/(d+m)$ represents the effect of the biological detritus reaching the deep ocean compared to the deep mixing and the general circulation. Finally, the term $[P/(d+u)]\,[P/(d+m)]$ in (9b) represents the effect of the ocean circulation on the nutrient and carbon distribution in intermediate versus deep waters, as seen previously while discussing the nutrient maximum (cf. (5)).

With DOM, (9) is replaced by

pCO_2 "increases with"

$$- (r_c - (2\mu - 1)r_{ca} + \mu r_n)\frac{P}{d+u}\left[1 - \lambda\frac{d}{d+m}\right]$$
$$+ \lambda\left[(2\mu - 1)r_{ca}\varepsilon' - (r_c + \mu r_n)\varepsilon\right]\frac{P}{d+m} \qquad (10a)$$
$$- (r_c + \mu r_n)\, H(d,u,m)\, Q \ ,$$

where $H(d,u,m)$ is a rational function of d, u, m.We get:

pCO_2 "increases with"

$$- 105\ \frac{P}{d+u} + 105\ \lambda\frac{P}{d+u}\ \frac{d}{d+m}$$
$$- 0.5\ \lambda\ \frac{P}{d+m} - 118\frac{Q}{d+u} \qquad (10b)$$
$$+ 118\ \lambda\ (1-\lambda)\frac{d - \frac{v_3}{v_2}u}{d+m+\lambda\frac{v_2}{\tau}}\frac{Q}{d+u} \ ,$$

where we used the first order approximation

$$H(d,u,m) \sim \lambda\, G(d,u,m) + \frac{1}{d+u} \ . \qquad (11)$$

3. ATMOSPHERIC CO_2 AND THE DEEP CIRCULATION

3.1. *Effect of the General Circulation on pCO_2*

The role of the thermohaline turnover d in changing pCO_2 when no DOM is incorporated in the model can be deduced from (9a). Care is required in interpreting the role of the fraction $P/(d+u)$, since P is an increasing function of d (and u). In this simple three-box model, it can be shown (cf. Appendix B) that, independently of the parameterization used for P, the ratio $P/(d+u)$ will still decrease when u (or d) increases. This follows from the intuitive fact that, considering biological productivity as a carbon pump fed by the incoming nutrients carried by $(u + d)$, this pump cannot be more than 100% efficient. The fraction $P/(d+u)$ will therefore decrease, although it can remain close to constant, for a near-perfect efficiency.

The dominant effect of increasing d will consequently be to reduce the term $1 - \lambda\,[\,d/(d+m)\,]$ (which in fact means increasing the nutrient maximum in intermediate waters, as seen in section 3.2). This also illustrates the importance of intermediate waters in this discussion: if m is taken very large (no intermediate waters), this term tends to unity, and the deep circulation d acts on pCO_2 only through $P/(d+u)$; this action could very well be counterbalanced by the second term of (9a) that we have neglected or by what would happen in the polar box of a more realistic model.

Both $1 - \lambda\,[\,d/(d+m)\,]$ and $P/(d+u)$ tend to increase the pCO_2 when d increases. This is compatible with our qualitative knowledge of what happens during a glacial-interglacial transition, when thermohaline turnover is strengthened while the atmospheric pCO_2 grows. This growth, however, is too small in current models, motivating the examination of the quantitative role of DOM.

The additional terms due to DOM in (10b) are somewhat similar to those in (9b). The terms corresponding to $P/(d+u)$ and $P/(d+u)\ d/(d+m)$ for DOM which will behave the same way if we assume that DOM and particulate matter are produced in some constant proportion (Q/P). The dominant contribution will come from the two terms:

$$105\ \lambda\ \frac{P}{d+u}\ \frac{d}{d+m} \ ;$$

$$118\ \lambda\ (1-\lambda)\frac{d - \frac{v_3}{v_2}u}{d+m+\lambda\frac{v_2}{\tau}}\ \frac{Q}{d+u} \ ,$$

If we assume that P and Q are produced in some constant proportion, and that this production is strictly proportional to the incoming nutrients (i.e. proportional to $d+u$) then $P/(d+u)$ and $Q/(d+u)$ are constants, and the two expressions above are increasing functions of d. Consequently the introduction of DOM does not change the behavior of the system: pCO_2 will increase with increasing thermohaline overturning. But the rate of increase will be much smaller. Looking only at the first factors, for $\lambda \approx 0.75$, we get $105\ \lambda \approx 79$, and $118\ \lambda(1-\lambda) \approx 22$. From Figure 5 it is clear that the introduction of DOM, as anticipated, reduces the sensitivity of pCO_2 to changes in the deep circulation.

3.2. *Polar Regions*

While the three-box model is awkward in trying to describe specifically what happens in high latitudes, we can still use (9) and (10) in order to get some insight into the basic mechanisms. In this model, by taking a very large mixing m, the intermediate and the deep box will behave like one box, the surface layer has to be chosen thicker, u interpreted for the present purpose as the deep convection, and d defined with an opposite sign. Equation (10b), with m taken very large, tells us that DOM is irrelevant to the discussion here; the only remaining terms are $Q/(d+u)$ which is proportional to $P/(d+u)$, and $P/(d+u)$ itself. Accordingly, pCO_2 will behave like $-P/(-d+u)$: it will decrease when the deep convection u decreases, or when d increases. The effect of d in high latitudes is, not supprisingly (its sign being reversed), the opposite of its effect in low latitudes. Without intermediate waters, however, and the term $1 - \lambda\,[\,d/(d+m)\,]$ of (9a), changes of d in the polar regions will not dominate atmospheric pCO_2 changes.

3.3. *Summary of Analytical Results*

During a glacial-interglacial transition it is reasonable to assume that u decreases as a result of weakened mid-latitude winds and d increases as a result of enhanced deep-water formation. The resulting effect on atmospheric pCO_2 will be due mainly to the term $1 - \lambda\,[\,d/(d+m)\,]$ in (9a), which represents the stratification of the nutrient distribution between intermediate and deep waters. A weakening of this stratification, due for example to the advection of DOM, will result in a carbon cycle less sensitive to deep-ocean circulation changes. This corresponds to the intuitive idea that the presence of carbon-rich waters in the nutrient maximum, resulting from the rapid regeneration of falling particulate matter, can affect pCO_2 through the action of d or u. If part of this organic matter is advected as a dissolved compound instead of being regenerated in the first thousand meters, less DIC will be available near the surface and the atmospheric pCO_2 will be less sensitive to the circulation pattern.

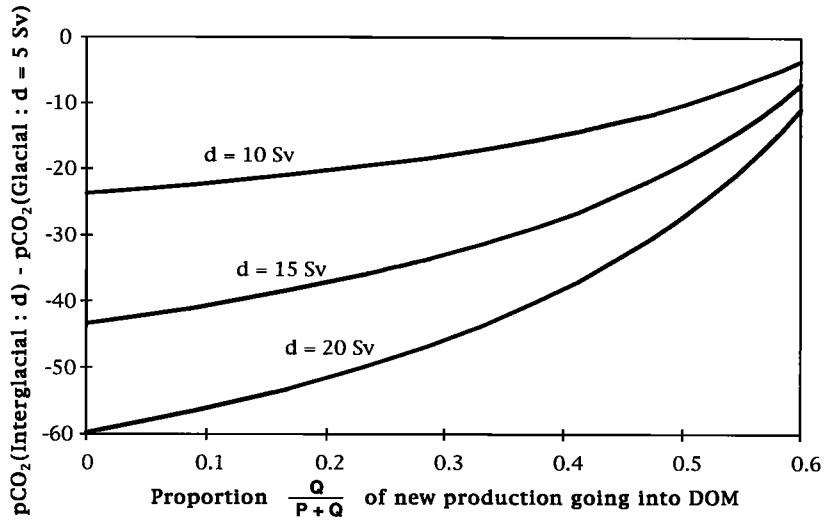

Fig. 5. Plot of the "glacial-interglacial" pCO_2 difference as a function of DOM production, where the glacial stage is defined here by $d = 5$ Sv. The efficiency of ocean circulation changes to modify pCO_2 is lowered by the presence of DOM.

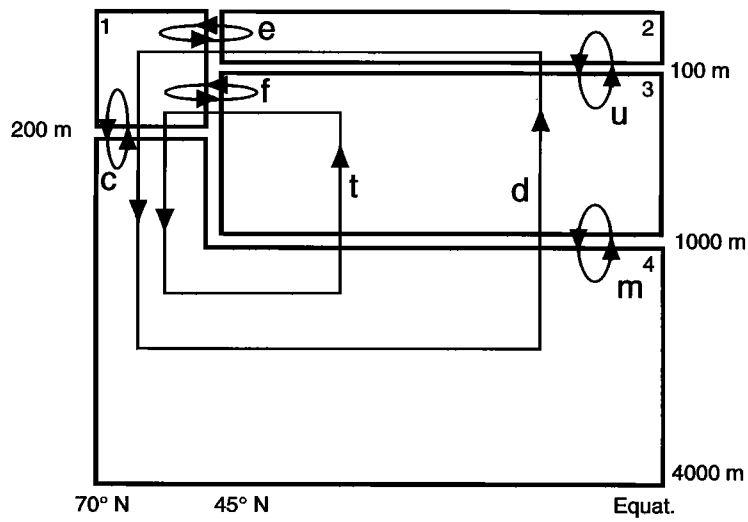

Fig. 6. Schematic diagram of the four boxes for the numerical model. Seven loops represent the oceanic circulation; their fluxes are given by d, t, u, m, c, e, and f. The new production (P_L in low latitudes, P_H in high latitudes) is parameterized in the same way as before. In high latitudes, all the production P_H goes to the deep box, as well as a fraction ε of P_L.

This simple three-box model is able, somewhat surprisingly, to reproduce the general behavior of the oceanic carbon cycle, but it cannot give acceptable numerical estimates of oceanic concentrations and consequently of atmospheric pCO_2. In order to obtain an estimate of the atmospheric CO_2 variation due to changes in the oceanic circulation, a more realistic model, (with an explicit calculation of pCO_2 and with a polar box), is developed in the next section.

4. A SIMPLE FOUR-BOX MODEL

4.1. *Model Description*

A more satisfactory representation of the oceanic carbon cycle is obtained by using four boxes: a high-latitude cold surface box and a low-latitude warm surface box represent respectively a sink and a source of atmospheric CO_2; an intermediate box, necessary to model the stratification of nutrients in the ocean, the importance of which was demonstrated in the previous chapter; and the deep box as the main reservoir. A schematic diagram of the boxes and of the fluxes between them is shown on Figure 6. There are seven independent loops describing the circulation and the mixing between the boxes: d and t represent the general thermohaline circulation, m the deep mixing, u the wind-driven upwelling, c the high-latitude deep convection, e the mixing between warm surface waters and cold surface waters, and f the mixing along isopycnals.

The advection scheme is the same as in the analytical model described in section 2: the water mass flux f_{ij} between a box i with a concentration C_i and a box j with a concentration C_j

transports a dissolved-matter flux $f_{ij} C_i$. The parameterization of the biological new production is given by the Michaelis-Menton formula, which we write here as a function of the nutrients in box number i ($i = 1$ or 2):

$$P_i = P_{max} \frac{N_i}{k_s + N_i} \quad . \tag{12}$$

The values of $P_{max} = 3$ molC m^{-2} yr^{-1} and of $k_S = 0.5$ μmolPO_4 L^{-1} are taken the same in the two surface boxes: the high nutrient content in the polar box ($i = 1$) is therefore the result of the deep convection c and of the mixing f with intermediate waters "along isopycnals." As in section 2, the Redfield ratios are $r_C = 106$, $r_{Ca} = 21$, and $r_n = 15$ and the remineralization and dissolution coefficients are $\varepsilon = 0.1$ and $\varepsilon' = 0.9$ (see Table 1).

4.2. *Glacial-Interglacial Transition*

First, the model is investigated in its simplest possible form, as described above. The effect that the seven circulation parameters u, c, d, t, f, e and m have on atmospheric pCO_2 and on the nutrient in intermediate waters is depicted in Figure 7. In the real ocean, high-latitude surface waters are fed essentially by thermocline water (t) and not by surface water (d). The high-latitude deepwater formation will therefore be carried mainly by the parameter t. In this diagram, variations of each parameter are shown and compared to a standard (glacial) state, defined by $e = 5$ Sv; $f = 10$ Sv; $c = 20$ Sv; $d = 5$ Sv; $m = 10$ Sv; $t = 20$ Sv; $u = 25$ Sv. The resulting equilibria are shown in the plane of atmospheric pCO_2 and nutrient content of the intermediate box. The concentrations in each box are given in Table 2 for the standard values of the circulation parameters.

For an interglacial-age scenario, stronger deepwater formation in high latitudes (t) than during a glacial age is a very reasonable assumption [Broecker et al., 1990; Shackleton et al., 1988]. This corresponds, during glacial stages, to the slow-down of Broecker's conveyor belt. Therefore a glacial-interglacial transition can be represented by an increase in t. We would also like to have higher upwelling rates u during glacial stages than today: in many coastal areas and in equatorial regions the productivity was probably higher then [Arrhenius, 1952; Mix, 1989; Sarnthein et al., 1987, 1988]; this is consistent with stronger winds associated with stronger temperature gradients.

The changes in the high-latitude convection c and in the "mixing" f are far from been so easily understood. Paleoproduction in high latitudes is poorly known, since the possible paleoproductivity indicators do not always agree. But not indicator suggests dramatic changes during glacial-interglacial transitions, for example Bareille's [1991] silica fluxes, while some suggest even a possible decrease [Labeyrie and Duplessy, 1985; Mortlock et al., 1991]. This could suggest lower values for c and f during a glacial stage, but ^{13}C isotopes do not agree with Cd/Ca results [Boyle, 1992] with respect to deep-water nutrient content, implying that we do not fully understand the geochemistry of the southern ocean in this time period.

Changes in e do not affect the results very much, and it is difficult to find physical phenomena able to produce considerable changes in m, which represents the diffusive mixing in the deep ocean. We then define a standard glacial-interglacial transition as an increase in t, a decrease in u and a small increase in c. Other possible transitions are also shown in Figure 7. As discussed in sections 2 and 3, all of them associate an increase in pCO_2 with an increase in the nutrient content of intermediate waters. This is mainly due to the circulation parameter t (cf. the discussion of d and pCO_2 in section 3.1), and illustrate well the relationship between atmospheric pCO_2 and the nutrient stratification. Oxygen and carbon isotopes have also been calculated for each set of parameters, and compare reasonably well with oceanic values.

The standard transition described here explains a 26.8 ppm atmospheric pCO_2 difference, which is far from the documented 80 ppm difference. A more realistic glacial-interglacial transition would probably involve variations in several other parameters. Since the system is only weakly nonlinear, a model with many more boxes would not give too different a result. It seems therefore that, within the context of this type of box model, changes in the oceanic circulation alone cannot

TABLE 1. Symbols and Their Numerical Values

Parameter	Value	Unit
	Volumes of the Four Boxes	
v_1	17	Mkm^3 (10^6 km^3)
v_2	26	Mkm^3
v_3	234	Mkm^3
v_4	1107	Mkm^3
	Areas of the Surface Boxes	
Σ_1	80.3	Mkm^2 (10^6 km^2)
Σ_2	265.9	Mkm^2
	Salinities and Temperatures	
s_1	33.75	‰
s_2	35.45	‰
t_1	4.5	°C
t_2	23.8	°C
	Exchange Velocity for CO_2	
E_1	0.11	molC m^{-2} yr^{-1}
E_2	0.07	molC m^{-2} yr^{-1}
	Mean Concentrations in the Sea	
A	2.4	meqAlk L^{-1}
N	2.145	μmolPO_4 L^{-1}
C	2.3	mmolDIC L^{-1}
	Redfield Ratios and Remineralization Coefficients	
r_C	106	
r_{Ca}	21	
r_n	15	
ε	0.1	
ε'	0.9	
	Michaelis-Menton Formula Parameter Values	
P_{max}	3	molC m^{-2} yr^{-1}
k_S	0.5	μmolPO_4 L^{-1}
	Oceanic Circulation	
d	5 - 10	Sverdrups (10^6 $m^3.s^{-1}$)
t	20 - 40	Sv
m	30 - 5	Sv
u	20 - 10	Sv
c	20 - 30	Sv
e	5 - 10	Sv
f	10 - 15	Sv

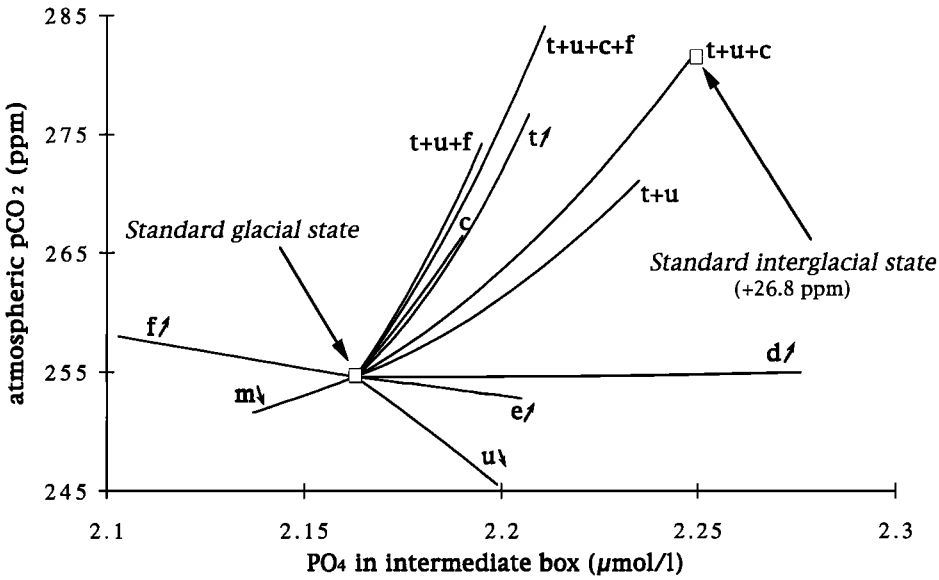

Fig. 7. Summary of four-box model results without DOM. Each line represents a change in the ocean circulation. A "standard" glacial-interglacial transition is defined by simultaneous changes in *t*, *u*, and *c*, and the interglacial atmospheric pCO_2 is 26.5 ppm higher.

explain the low carbon dioxide content of the atmosphere during the last glacial maximum. Other changes should be taken into account, mainly variations in the mean concentrations of nutrients, carbon and alkalinity. These are certainly not constant in the real world, because of sea level changes, as well as variations in river input and in sediment preservation.

4.3. *Comparison With Other Box Models*

We have chosen here to study the effect of oceanic-circulation changes alone, everything else being held constant. This accounts for some of the differences with some other simple box models.

In the work by Knox and McElroy [1984], the new production in high latitude is increased arbitrarily by a factor of 100. In the work by Sarmiento and Toggweiler [1984] and in the work by Siegenthaler and Wenk [1984], the high-latitude production P_h is an independent parameter, and large pCO_2 variations are obtained when increasing P_h (in the former) or keeping it constant (in the latter), while decreasing the high-latitude convection *c*. Here P_h is calculated as a function of the nutrient content, itself a function of the circulation, and it increases with increasing *c*. In addition, the circulation parameters are changed at most by a factor of two. The large pCO_2 variations found in these earlier papers are therefore ruled out here.

The model of Marino et al. [1992] (published while this paper was under review) is an extension of Knox and McElroy model. Though the circulation parameters are allowed to differ from present-day values much more than here (deepwater formation is totally supressed and intermediate-water formation is multiplied by six for the glacial stage) the resulting pCO_2 variations (31 ppm) are similar to the results of our model.

TABLE 2. Concentrations for the Standard Glacial and Interglacial Circulation in the Absence of DOM

Parameter	Box	Glacial	Interglacial	Unit
pCO_2 atmosphere		254.6	281.4	ppm
Phosphate	1	1.033	1.398	μmol L^{-1}
	2	0.149	0.097	
	3	2.163	2.248	
	4	2.205	2.183	
Production	1	2.021	2.210	molC m^{-2} yr^{-1}
	2	0.689	0.488	
Alkalinity	1	2.356	2.372	meq L^{-1}
	2	2.323	2.333	
	3	2.376	2.389	
	4	2.408	2.404	
Oxygen	1	319.5	319.3	μmol L^{-1}
	2	215.5	215.5	
	3	53.6	135.8	
	4	94.3	177.4	
Carbon	1	2.133	2.168	mmol L^{-1}
	2	1.936	1.965	
	3	2.246	2.268	
	4	2.281	2.271	
pCO_2	1	248.3	279.1	ppm
	2	257.6	282.5	
Carbon 13	1	1.44	1.03	per mil
	2	2.15	1.76	
	3	0.002	-0.063	
	4	0.044	0.090	
^{13}C atmosphere		-5.97	-6.37	per mil
$\Delta^{14}C$	1	-75.8	-83.3	per mil
	2	-37.0	-26.1	
	3	-118.9	-121.6	
	4	-141	-129.1	

Much larger variations of pCO_2 are achieved, however, by these authors when changing the global budget of nutrients, carbon and alkalinity, and changing the coefficients of the biological parameterization.

4.4. *Effect of Dissolved Organic Matter*

As mentioned earlier, a new method for measuring dissolved organic matter (DOM) has given several times the amounts found by traditional methods [Sugimura and Suzuki, 1988]. Yet nobody else has reported similar results and these measurements remain controversial. According to these authors, this DOM pool shows marked variations with depth, suggesting that it is actively involved in the transport of carbon, while the DOM fraction already known from older measurement methods is very long-lived (several thousands of years) and consequently more or less uniformly distributed in the ocean [Williams and Druffel, 1987]. In order to exhibit a strong gradient between 300 and 500 m as found by Sugimura and Suzuki, this new DOM must be more labile and be regenerated with a characteristic time of the order of a century.

The addition of the new, larger and more rapidly-recycled DOM pool into the model is straightforward: the production of DOM is considered to represent 50% of the new production, which is then advected by the water and slowly transformed back into inorganic matter through biological consumption, with an exponential decay time constant of 200 years. Simulations with the same parameter values as in the DOM-free case give the results summarized in Figure 8. The concentrations in each box are given, for the standard states, in Table 3. We notice that the nutrient content is much lower than in the no-DOM situation: the effect of DOM is to smooth the action of the biology. This was also noticed in GCM simulations of the present ocean [Bacastow and Maier-Reimer, 1991], which show a smaller nutrient maximum in the equatorial intermediate waters, in better agreement with in situ measurements. The addition of DOM in these GCM simulations also leads to disappearance of an unwanted anoxic region in the intermediate equatorial waters. In our model, the low-latitude region is much too wide to represent the equatorial zone only and no anoxia is observed, but we note that the oxygen level increases in intermediate waters when DOM is incorporated, which is a corollary of the reduction in nutrient content.

In the presence of DOM the geochemical stratification of the ocean is weakened, and as a result the pCO_2 variations between the different circulation regimes are smaller: the standard transition allows a 15.3 ppm pCO_2 difference and, from the figure, it is clear that alternate scenarios would give similar results. This smoothing effect depends only weakly on the exact parametrization of DOM: if a bigger fraction of the new production is transformed into DOM, or if we take a longer time constant for the decay into inorganic matter, the smoothing action of DOM increases, while opposite assumptions lead to a DOM decrease. This means that the smoothing effect depends mainly on the size of the DOM pool in the ocean. If this pool is not negligible, then it makes the size of pCO_2 glacial-interglacial differences more difficult to explain.

Our model results appear to be quite robust: the diagrams are very similar in both cases, with changes in the oceanic circulation having more or less the same effects. Many different possible parameterizations of the biological component of the system have been tried, nonlinear formulas for the new production, for the regeneration of the falling particulate matter, etc., without changing the general behavior described in the "standard case." Models with more boxes have also been explored, but the main results given here do not seem to depend on the geographic details that would be provided by a more realistic model.

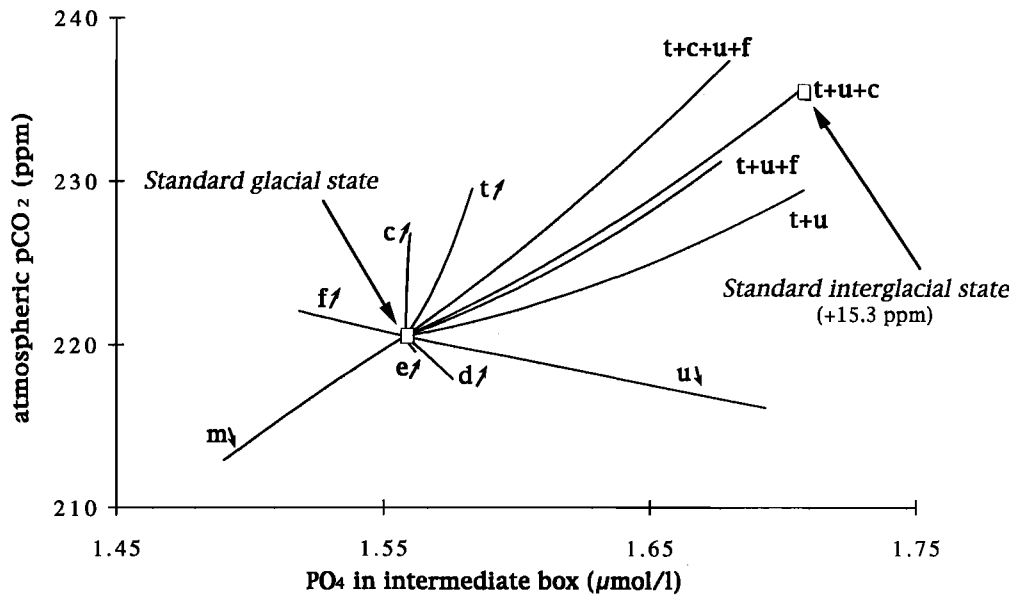

Fig. 8. Same as Figure 7, but when DOM is incorporated in the model. Nutrient levels are much lower in the intermediate box than previously and the resulting atmospheric pCO_2 difference smaller.

TABLE 3. Concentrations for the Two Standard Circulations with the Introduction of DOM

Parameter	Box	Glacial	Interglacial	Unit
pCO_2 atmosphere		220.5	235.8	ppm
Phosphate	1	0.697	1.011	$\mu mol\ L^{-1}$
	2	0.105	0.075	
	3	1.558	1.708	
	4	1.746	1.738	
Production	1	1.747	2.007	$molC\ m^{-2}\ yr^{-1}$
	2	0.521	0.393	
DOM (PO_4)	1	0.979	0.801	$\mu molDOP\ L^{-1}$
	2	1.272	1.235	
	3	0.587	0.475	
	4	0.425	0.424	
Alkalinity	1	2.382	2.388	$meq\ L^{-1}$
	2	2.371	2.373	
	3	2.391	2.396	
	4	2.403	2.402	
Oxygen	1	320.1	320.0	$\mu mol\ L^{-1}$
	2	215.4	215.4	
	3	113.8	169.7	
	4	121.4	190.0	
Carbon	1	2.125	2.147	$mmol\ L^{-1}$
	2	1.942	1.957	
	3	2.188	2.216	
	4	2.236	2.230	
pCO_2	1	211.6	230.7	ppm
	2	224.8	238.2	
Carbon 13	1	1.34	1.05	per mil
	2	1.99	1.78	
	3	0.193	0.107	
	4	0.169	0.205	
^{13}C atmosphere		-6.11	-6.36	per mil
$\Delta^{14}C$	1	-82.5	-93.1	per mil
	2	-41.7	-31.4	
	3	-124.6	-130.3	
	4	-146.9	-138.2	

5. SUMMARY AND CONCLUSIONS

Two types of extremely simplified oceanic carbon cycle models have been presented: an analytic three-box model (sections 2 and 3) and a numerical four-box model (section 4). The simple formulas obtained from the analytic model provide useful insight into the influence of the oceanic circulation on the carbon stratification of the ocean, and ultimately on atmospheric pCO_2 . The low CO_2 level during the last glacial maximum could be the result of a slowdown of the thermohaline circulation or of weaker deep convection in polar areas; but as long as the new production is an increasing function of the nutrients, stronger upwelling at low latitudes should, on the contrary, increase the atmospheric CO_2 concentration.

The numerical four-box model yields a more quantitative estimate of the changes in the oceanic carbon cycle associated with changes in the circulation. The main result is that a paleoceanographic circulation pattern compatible with what we know about the glacial ocean cannot explain an atmospheric pCO_2 level 80 ppm lower than in preindustrial time, and that the introduction of dissolved organic matter (DOM) into the system only makes the explanation even more difficult. If the DOM pool is negligible, we can at best explain a 30 ppm difference, with a more probable value between 10 and 20 ppm, and the presence of DOM reduces this effect by as much as 50%.

The carbonate response of the sediment could perhaps provide us with another 10 or 20 ppm [Boyle, 1988], but this would still be insufficient. This is entirely consistent with ocean GCM experiments [Heinze et al., 1991] which take into account some simple interactions with the sediment and give a pCO_2 difference of 28 ppm between the present and a glacial-age ocean circulation. Numerous hypotheses have been formulated in order to account for such a discrepancy between the models and the paleoclimatic data; most of them involve increased biological production at high latitudes, the last one being the fertilization of polar oceans by iron [Martin and Fitzwater, 1988; Martin et al., 1990]. Reconstructions of paleoproductivity, however, are in disagreement with a large-scale increase in productivity in polar regions [Labeyrie and Duplessy, 1985; Mortlock et al., 1991], and no indication of anoxia, as would be implied by the high productivity levels required by such mechanisms, is to be found in those regions during the last glaciation.

In addition, recent measurements of ^{13}C in the carbon dioxide trapped in air bubbles from Antarctic ice [Leuenberger et al., 1992], as well as plant analysis [Marino et al., 1992], indicate that atmospheric ^{13}C was probably lower during the last glacial maximum. Keir [1992] argues convincingly this makes it more difficult to account for the lower atmospheric pCO_2 at that time, because increasing ocean productivity and, to a smaller extent, reducing the nutrient maximum through changes in ocean circulation as done in this paper, also increases surface water and atmospheric ^{13}C. Furthermore, Keir [1991] used a three-box model and a 13-box model to show that an increase in the biological carbon pump efficiency requires a considerable reduction of the amount of land biota to account for lower ^{13}C in the deep ocean. Hence the decrease in intermediate-depth nutrients during glacial time may be better explained by changes in the ocean circulation or in the biological recycling.

It is conceivable that some crucial elements of the oceanic carbon budget have been overlooked, like $CaCO_3$ sedimentation or river inputs; it may also be that our representation of the biological processes coupled with the mixed-layer dynamics is oversimplified [Simonot et al., 1988]. In any case the changes in ocean circulation studied in this paper are not sufficient to explain the lower pCO_2 level of the last glacial maximum, and dissolved organic matter makes matters only more difficult. Still, we hope that the analytical and numerical methodology developed here to explore the parameter space of the ocean's biochemistry will help in the eventual resolution of the glacial-interglacial pCO_2 dilemna.

While the present paper was under review, Suzuki [1993] has renounced his earlier claims and the existence of a large pool of labile DOM seems therewith more hypothetical. In the light of our modeling results, this new report comes as a relief. Though still acting as a smoother on the spatial and temporal variations of inorganic carbon in the sea, as discussed in our paper, the small amounts of labile DOM can probably be

neglected in a first approximation of the oceanic carbon cycle model. Although the glacial-interglacial pCO_2 problem remains unsolved, the additional difficulties involved by dissolved organic matter probably do not exacerbate the situation.

APPENDIX A: SOLUTION OF THE THREE-BOX MODEL WITH DOM.

The best way to solve (1), (3), and (4) is use the variables $(N_i - D_i)$, $(A_i - r_n D_i)$ and $(C_i + r_c D_i)$ that are solutions of (2). We then obtain directly:

$$N_2 - N_3 = (\text{terms without DOM}) - (D_2 - D_3)$$

$$pCO_2 \approx [(C_1 - A_1) - (C - A)]/(v_2 + v_3)$$

$$\approx (\text{terms without DOM}) - (r_c + r_n)(D_1 - D)/(v_2 + v_3)$$

with $D = v_1 D_1 + v_2 D_2 + v_3 D_3$ being the mean DOM concentration.

To solve (3), we can use the intermediate variables $D_{13} = D_1 - D_3$, $D_{23} = D_2 - D_3$. We then obtain the system of two equations with two unknowns:

$$\left(\frac{v_3}{\tau} u - \frac{v_2}{\tau} d\right) D_{13} = \left[\frac{v_2}{\tau}(m + \frac{v_3}{\tau}) + \frac{v_3}{\tau}(m + d + u)\right] D_{23}$$

$$\left[\frac{v_3}{\tau}(u + d + \frac{v_1}{\tau}) + \frac{v_1}{\tau} d\right] D_{13} = \left[\frac{v_3}{\tau}(d + u) - \frac{v_1}{\tau} m\right] D_{23} + \frac{v_3}{\tau} Q$$

Its solution is

$$D_{23} = \frac{v_3}{\tau}\left(\frac{\frac{v_3}{\tau} u - \frac{v_2}{\tau} d}{\Delta}\right) Q$$

$$D_{13} = \frac{v_3}{\tau}\left(\frac{\frac{v_2}{\tau}\left(m + \frac{v_3}{\tau}\right) + \frac{v_3}{\tau}(d + m + u)}{\Delta}\right) Q$$

with

$$\Delta = \left(\frac{v_2}{\tau}\right)^2 \left[d^2 + m\,d + m\,u + d\,u + \frac{v_1}{\tau}(m + d + u)\right] + \frac{v_3}{\tau}\frac{v_2}{\tau}\left[d^2 + m\,d + m\,u + d\,u + \frac{v_3}{\tau}(\frac{v_1}{\tau} + d + u) + \frac{v_1}{\tau} m\right] + \frac{v_3}{\tau}\frac{v_1}{\tau}\left(d^2 + m\,d + m\,u + d\,u\right) + \frac{v_3}{\tau}\frac{v_2}{\tau}\frac{v_1}{\tau} m\,.$$

To simplify this expression, we notice that v_1 is negligible compared to v_3. We can therefore use the approximate expression:

$$\Delta = \left(\frac{v_3}{\tau}\right)^2 (d + u)\left(\frac{d + m}{\lambda} + \frac{v_2}{\tau}\right)$$

The functions $G(d,u,m)$ and $H(d,u,m)$ introduced in Section 2 are given as functions of D_{13} and D_{23} by

$$G = D_{23} / Q\,,$$

$$H = [(D_{13} - D_{23}) + \lambda D_{23}] / Q = \frac{1}{d + u} + \lambda G\,.$$

This yields (7) and (11) used in sections 2 and 3.

APPENDIX B: EFFECT OF PRODUCTIVITY AND UPWELLING IN THE THREE-BOX MODEL.

Using Broecker and Peng's [1982] Redfield ratios, and assuming that m is of the same order of magnitude as d (^{14}C calibration of numerous box models suggests that m might actually be 2 or 3 times larger than d), it follows from (9) that $d/(d+m)$ is of the order of (or smaller than) one half. This means that the dominant term of the right-hand side of (9b) is clearly the first one, and to zeroth order, pCO_2 will behave like $P/(d+u)$. An increase in productivity without any change in the ocean circulation does decrease the pCO_2. An increase in the upwelling rate u must be looked at more carefully, because P itself depends on the circulation. However, in the realm of this simple three-box model, it can be shown that, independently of the parameterization used for P, the ratio $P/(d+u)$ will still decrease when u (or d) increases. This is actually the result of the quite intuitive idea that biology, considered as a carbon pomp fed by the incoming nutrients carried by $(u + d)$, cannot be more than 100% efficient.

This implication can be easily verified using either a crude parametrization for P, like $P = \mu(d+u)N_2$, i.e., the production is proportional to the incoming nutrients (for $\mu=1$, there are no nutrients left in the surface box), or a more realistic one like the Michaelis-Menton formula:

$$P = P_{max} \frac{N_1}{k_s + N_1}$$

[Dugdale, 1967] and then solving the resulting equations (1a), (2a), and (2b), of the first or the second degree accordingly. More generally, if we assume that P is a function of N_1 only, increasing with N_1, then, from the solution of (1a), (2a), and (2b), we have $\partial N_1/\partial u$ and $\partial N_2/\partial u$ as functions of $\partial P/\partial u = (dP/dN_1)\,\partial N_1/\partial u$. We can therefore obtain $\partial(N_2-N_1)/\partial u$ as a function of dP/dN_1 only, and from (5a) deduce that $P/(d+u)$ will decrease when u increases:

$$\frac{\partial\left(\frac{P}{d+u}\right)}{\partial u} = -\frac{P}{(d+u)^2} \frac{1 + v_3\left(\frac{\varepsilon}{d+m}\right)\frac{dP}{dN_1}}{1 + \left[\frac{v_3}{d+m}\left(\varepsilon + \frac{m}{d+u}\right) + \frac{v_2}{d+u}\right]\frac{dP}{dN_1}}$$

On the other hand, if the deep mixing m is small enough compared to d, then the factor $1 - \lambda\,[\,d/(d+m)\,]$ can be as low as $1 - \lambda \approx 0.25$ and the two terms on the right-hand side of (5a) are of the same order of magnitude. Even in this case, some dramatic assumptions have to be made on ε and ε' in order to reduce pCO_2 by increasing u. Boyle [1986] succeeds in doing so in a four-box model, by taking $\lambda = 0.87$, $m = 0$, and $\varepsilon = \varepsilon' = 0.2$. However, in a box model having diffusive mixing between the deep and intermediate box, it seems hopeless to obtain a reduction in atmospheric CO_2 by an increase in upwelling, as is supposed to have occured during glacial maxima due to an intensification of the pole-to-equator temperature difference and hence of the zonal winds.

Acknowledgments. It is a pleasure to acknowledge seminal discussions with J.-C. Duplessy and L. Labeyrie. Most of this work was carried out while D. Paillard was visiting the Department of Atmospheric Sciences and Institute of

Geophysics and Planetary Physics at UCLA. It was supported by NSF grant ATM 90-13217 (D. Paillard and M. Ghil), by an NSF Special Creativity Award (M. Ghil) and by additional support from PNEDC/INSU and CEA (D. Paillard). This is CFR contribution 1387.

REFERENCES

Arrhenius, G., Sediment cores from the East Pacific, Swedish Deep-Sea Expedition 1947-1948, *Rep. 5*, pp. 1-228, 1952.

Bacastow, R., and E. Maier-Reimer, Dissolved organic carbon in modelling oceanic new production, *Global Biogeochem. Cycles, 5,* 71-85, 1991.

Bareille, G., Flux sédimentaires: Paléoproductivité et paléocirculation de l'océan austral au cours des 150 000 dernières années, Ph. D. thesis, Univ. de Bordeaux, Bordeaux, France, 1991.

Barnola, J. M., D. Raynaud, Y. S. Korotkevich, and C. Lorius, Vostok ice core provides 160,000-year record of atmospheric CO_2, *Nature, 329,* 408-414, 1987.

Berger, W. H., V. S. Smetacek, and G. Wefer, Ocean productivity and paleoproductivity - An overview, in *Productivity of the Ocean: Past and Present*, edited by W. H. Berger et al., pp. 1-34, John Wiley, New York, 1989.

Boyle, E. A., Deep ocean circulation, preformed nutrients, and atmospheric carbon dioxide: Theories and evidence from oceanic sediments, in *Mesozoic and Cenozoic Oceans*, Geodyn. Ser., vol. 15, edited by K.J. Hsü, pp. 49-59, AGU, Washington D. C., 1986.

Boyle, E. A., The role of vertical chemical fractionation in controling late Quaternary atmospheric carbon dioxide, *J. Geophys. Res., 93,* 15,701-15,714, 1988.

Boyle, E. A., Cadmium and $\delta^{13}C$ paleochemical ocean distributions during the stage 2 glacial maximum, *Annu. Rev. Earth Planet. Sci., 20,* 245-287, 1992.

Boyle, E. A., and L. D. Keigwin, Deep circulation of the North Atlantic over the last 200,000 years: Geochemical evidence, *Science, 218,* 784-787, 1982.

Broecker, W. S., and T. H. Peng, *Tracers in the Sea*, 690 pp., Eldigio, Palisades, N. Y., 1982.

Broecker, W. S., T. H. Peng, S. Trumbore, G. Bonani, and W. Wolfli, The distribution of radiocarbon in the glacial ocean, *Global Biogeochem. Cycles, 4,* 103-117, 1990.

Curry, W. B., and G. P. Lohmann, Reduced advection into Atlantic deep eastern basins during last glacial maximum, *Nature, 306,* 577-580, 1983.

Delmas, R. J., J. M. Ascencio, and M. Legrand, Polar ice evidence that atmospheric CO_2 20,000 BP was 50% of present, *Nature, 284,* 155-157, 1980.

Dugdale, R. C., Nutrient limitation in the sea: Dynamics, identification and significance, *Limnol. Oceanogr., 12,* 685-695, 1967.

Duplessy, J. C., N. J. Shackleton, R. G. Fairbanks, L. D. Labeyrie, D. Oppo, and N. Kallel, Deepwater source variations during the last climatic cycle and their impact on the global deepwater circulation, *Paleoceanography, 3,* 343-360, 1988.

Ghil, M., A. Mullhaupt, and P. Pestiaux, Deep water formation and Quaternary glaciations, *Clim. Dyn., 2,* 1-10, 1987.

Heinze, C., E. Maier-Reimer, and K. Winn, Glacial pCO_2 reduction by the world ocean: Experiments with the Hamburg carbon cycle model, *Paleoceanography, 6,* 395-430, 1991.

Kallel, N., L. D. Labeyrie, A. Juillet-Leclerc, and J. C. Duplessy, A deep hydrological front between intermediate and deep-water masses in the glacial Indian Ocean, *Nature, 333,* 651-655, 1988.

Keir, R. S., On the Late Pleistocene ocean geochemistry and circulation, *Paleoceanography, 3,* 413-446, 1988.

Keir, R. S., The effect of vertical nutrient redistribution on surface ocean $\delta^{13}C$, *Global Biogeochem. Cycles, 5,* 351-358, 1991.

Keir, R. S., Packing away carbon isotopes, *Nature, 357,* 445-446, 1992.

Knox, F., and M. B. McElroy, Changes in atmospheric CO_2: Influence of the marine biota at high latitude, *J. Geophys. Res., 89,* 4629-4637, 1984.

Labeyrie, L. D., and J. C. Duplessy, Changes in the oceanic $^{13}C/^{12}C$ ratio during the last 140,000 years: High-latitude surface records, *Palaeogeogr. Palaeoclimatol. Palaeoecol., 50,* 217-240, 1985.

Leuenberger, M., U. Siegenthaler, and C. Langway, Carbon isotope composition of atmospheric CO_2 during the last ice age from an Antarctic ice core, *Nature, 357,* 488-490, 1992.

Lyle, M., and N. Pisias, Ocean circulation and atmospheric CO_2 changes: Coupled use of models and paleoceanographic data, *Paleoceanography, 5,* 15-41, 1990.

Maier-Reimer, E., and K. Hasselmann, Transport and storage of CO_2 in the ocean - An inorganic ocean-circulation carbon cycle model, *Clim. Dyn., 2,* 63-90, 1987.

Marino, B., M. McElroy, R. Salawitch, and W. Spaulding, Glacial-to-interglacial variations in the carbon isotopic composition of atmospheric CO_2, *Nature, 357,* 461-466, 1992.

Martin, J. H., and S. E. Fitzwater, Iron deficiency limits phytoplankton growth in the north-east Pacific subarctic, *Nature,* 341-343, 1988.

Martin, J. H., R. M. Gordon, and S. E. Fitzwater, Iron in Antarctic waters, *Nature, 345,* 156-158, 1990.

Michel, E., L'océan au dernier maximum glaciaire: le cycle du carbone et la circulation. Contraintes isotopiques et modélisation, Ph. D. thesis, Univ. de Paris-Sud, 1992.

Mix, A. C., Influence of productivity variations on long-term atmospheric CO_2, *Nature, 337,* 541-544, 1989.

Mortlock, R. A., C. D. Charles, P. N. Froelich, M. A. Zibello, J. Saltzman, J. D. Hays, and L. H. Burckle, Evidence for lower productivity in the Antarctic Ocean during the last glaciation, *Nature, 351,* 220-223, 1991.

Quon, C., and M. Ghil, Multiple equilibria in thermosolutal convection due to salt-flux boundary conditions, *J. Fluid Mech., 245,* 449-483, 1991.

Sarmiento, J. L., and J. R. Toggweiler, A new model for the role of the oceans in determining atmospheric pCO_2, *Nature, 308,* 621-624, 1984.

Sarnthein, M., K. Winn, and R. Zahn, Paleoproductivity of

oceanic upwelling and the effect on atmospheric CO_2 and climatic change during deglaciation times, in *Abrupt Climatic Change*, edited by W. H. Berger and L. D. Labeyrie, pp. 311-337, D. Reidel, Norwell, Mass., 1987.

Sarnthein, M., K. Winn, J. C. Duplessy, and M. R. Fontugne, Global variations of surface ocean productivity in low and mid latitudes: Influence on CO_2 reservoirs of the deep ocean and atmosphere during the last 21,000 years, *Paleoceanography, 3,* 361-399, 1988.

Shackleton, N. J., J. C. Duplessy, M. Arnold, P. Maurice, M. A. Hall, and J. Cartlidge, Radiocarbon age of last glacial Pacific deep water, *Nature, 335,* 708-711, 1988.

Siegenthaler, U., and T. Wenk, Rapid atmospheric CO_2 variations and ocean circulation, *Nature, 308,* 624-627, 1984.

Simonot, J. Y., E. Dollinger, and H. Le Treut, Thermodynamic-biological-optical coupling in the oceanic mixed layer, *J. Geophys. Res., 93,* 8193-8202, 1988.

Stommel, H. M., Thermohaline convection with two stable regimes of flow, *Tellus, 13,* 224-230, 1961.

Sugimura, Y., and Y. Suzuki, A high-temperature catalytic oxydation method for the determination of non-volatile dissolved organic carbon in seawater by direct injection of a liquid sample, *Mar. Chem., 24,* 105-131, 1988.

Suzuki, Y., On the measurement of DOC and DON in seawater, *Mar. Chem., 41,* 287-288, 1993.

Thual, O., and J. C. McWilliams, The catastrophic structure of thermohaline convection in a two-dimensional fluid model and a comparison with low-order box model, *Geophys. Astrophys. Fluid Dyn., 64,* 67-95, 1992.

Toggweiler, J. R., Is the downward dissolved organic matter flux important in carbon transport?, in *Productivity in the Ocean: Present and Past (Dahlem Konferenzen)*, edited by W. H. Berger, V. S. Smetacek and G. Wefer, pp. 65-83, John Wiley, New York, 1989.

Welander, P., Thermohaline effects in the ocean circulation and related simple models, in *Large-scale Transport Processes in the Oceans and Atmosphere*, edited by J. Willebrand and D. T. L. Anderson, pp. 163-200, D. Reidel, Norwell, Mass., 1988.

Williams, P. M., and E. R. M. Druffel, Radiocarbon in dissolved organic matter in the central North Pacific Ocean, *Nature*, 246-248, 1987.

M. Ghil, Department of Atmospheric Sciences and Institute of Geophysics and Planetary Physics, University of California, Los Angeles, CA 90024.

H. Le Treut, Laboratoire de Météorologie Dynamique, Ecole Normale Supérieure, 24 rue Lhomond, F-75005, Paris.

D. Paillard, Laboratoire de Modélisation du Climat et de l'Environnement, CEA-DSM, Centre d'études de Saclay, Orme des Merisiers, Gif sur Yvette, F-91191, France.

(Received March 6, 1992;
revised July 6, 1993;
accepted July 22, 1993.)